Chiral Organocopper Electrocatalyst-Enabled Oxidative Kinetic Resolution of Primary Alcohols

Pei-Sen Gao, Hui-Lin Liu, You-Liang He, Ke-Jin Jiao, Cong Ma, Tian-Sheng Mei*

Key Laboratory of Organometallic Chemistry, Center for Excellence in Molecular Synthesis, Shanghai Institute of Organic Chemistry, University of Chinese Academy of Sciences, Chinese Academy of Science, Shanghai 200032, China.

*Corresponding author. Email: mei7900@sioc.ac.cn

Abstract

Asymmetric electrocatalysis is poised to provide a unique avenue for access to enantioenriched molecules that are difficult to obtain through more conventional approaches, but the development of efficient electrocatalysts capable of highly enantioselective transformations remains elusive. Towards this enviable end, bifunctional electrocatalyst capable of both redox mediation and delivery of high stereocontrol is needed. Here we disclose a novel TEMPO-BOX-ligated copper electrocatalyst that enables oxidative kinetic resolution of racemic 1,4-diols, affording diverse chiral 1,4-diols and γ-lactones with good or excellent chemo-, regio, and enantioselectivity. We also show that this cooperative Cu/TEMPO-BOX catalytic strategy is applicable to the electro-oxidative kinetic resolution of 1,2- and 1,3-amino alcohols. This work demonstrates the potential of bifunctional electrocatalysis for asymmetric synthetic methods and we anticipate that it will spur the development of new hybrid electrocatalysts to realize novel asymmetric electrocatalytic methods.

Electrocatalysis has emerged as a promising and sustainable tool for forging carbon–carbon and carbon–heteroatom bonds(*1-3*) since electric current serves as the sole traceless "reagent" for oxidation and reduction of organic and organometallic molecules. Furthermore, the ease of precise regulation of the electrical potential offers a convenient and underutilized handle for taming redox transformation.(*4-16*) In this context, the use of redox mediators such as TEMPO and other N-oxyl radicals to achieve indirect electrolysis offers great advantages compared to direct electrolysis in that electrode passivation is avoided, the delivered electrical potential is dampened, and functional group tolerance is enhanced.(*17-19*) The advancement of asymmetric electrochemical catalytic methods for accessing enantioenriched molecules has garnered broad interest across the organic synthesis community in recent years.(*20-23*) Owing to the versatile reactivity of transition metals and the ease of tailoring chiral ligands, the synergistic use of transition metal catalysis and redox mediators is an appealing strategy that could be merged under an umbrella of 'asymmetric

electrochemical catalysis'.(*24-31*) To achieve such a merger, the redox mediators should efficiently oxidize (or reduce) the substrate into a reactive intermediate that immediately enters an asymmetric catalytic cycle. Unfortunately, the presumably highly reactive oxidized (or reduced) intermediates are prone to diversion to side reactions that ultimately attenuate the efficacy of the electrocatalyst (Fig. 1A). Additionally, the reconciliation of multiple oxidation and reduction processes in metal catalysis could result in low efficiency and enantioselectivity, along with the deactivation of the metal catalyst by cathodic reduction. Inspired by Stahl's pioneering work on (bpy)Cu/TEMPO cooperative catalytic system for efficient oxidation of alcohols(*32*, *33*) and Meggers' work on substrates binding strategy for electrorhodium-catalyzed radical couplings,(*34*) we envisioned that a "two in one" strategy(*35-37*) involving an electrocatalyst bearing both a TEMPO mediator and a source of chirality within a single ligand could enable asymmetric electrochemical catalysis. Directly linking the redox mediator to the metal catalyst could minimize side-reactions by shortening the distance between the metal complex, redox mediator, and reactive intermediates and thereby maximize cooperativity to deliver the desired reaction outcome (Fig. 1B).

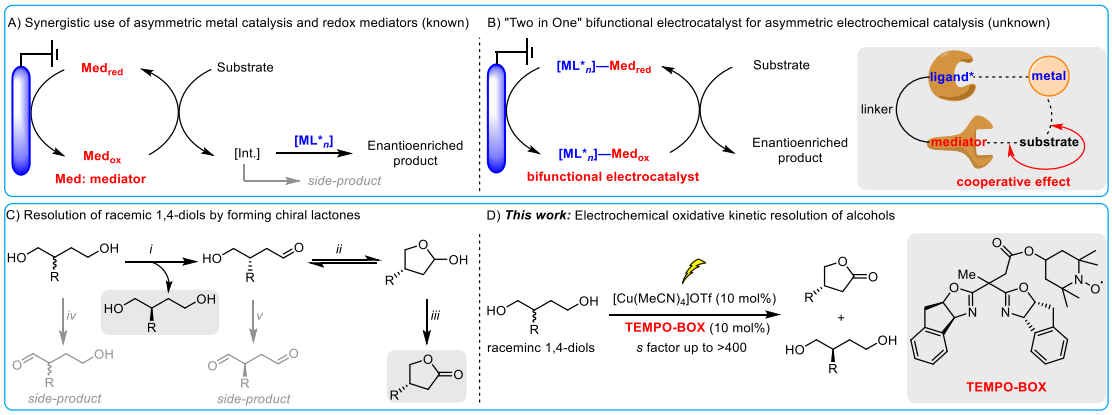

Fig. 1. Strategies for asymmetric electrochemical catalysis. A, Established strategy. B, Desired strategy. C, Resolution of racemic 1,4-diols by forming chiral lactones. D, This study.

We chose oxidative lactonization of 1,4-diols as a model reaction to test this hypothesis since chiral lactones are important structural motifs in natural products and pharmaceuticals, and are building blocks for the production of fine chemicals.(*38-42*) There are important fundamental challenges associated with an enantioselective electrochemical oxidative lactonization of 1,4-diols via kinetic resolution that make it an important benchmark reaction (Fig. 1C). First, selective oxidation of one of two primary alcohols can be difficult (i.e., competition between step *i* and step *iv*). Second, selective oxidation of the hemiacetal (lactol) over a primary alcohol presents another challenge (competition between step *iii* and step *v*). Finally, as with any kinetic resolution, achieving a high selectivity factor is required for utility. Herein, we describe the design and development of a bifunctional TEMPO-BOX ligand to enable electrochemical Cu-catalyzed lactone-forming kinetic resolution of 1,4-diols in an

undivided cell proceeding with high chemo-, regio-, and enantioselectivity (Fig. 1D). Examples of kinetic resolutions of amino alcohols are also provided.

Table 1. Reaction optimization.

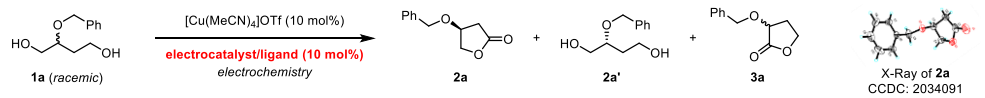

entry[a]	electrocatalyst/ligand	r.r of 2a/3a[b]	2a		2a'		s[e]
			yield (%)[c]	ee (%)[d]	yield (%)[c]	ee (%)[d]	
1	4/L1	>95:5	49	20	50	6	2
2	4/L2	88:12	24	67	73	12	6
3	4/L3	>95:5	53	-78	45	-60	15
4	4/L4	92:8	37	80	60	31	12
5	E1	>95:5	49(43)[f]	93	49(41)[f]	92	92
6	E2	>95:5	23(20)[f]	84	77(71)[f]	81	28
7	E3	>95:5	47	91	52	82	56
8	E4	>95:5	35	17	63	10	1
9	E5	>95:5	46	-72	51	-68	12

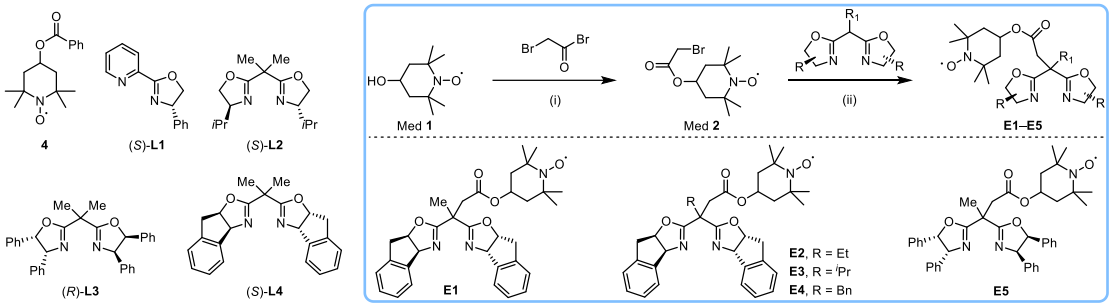

[a]Unless otherwise indication, the reaction was performed at 0.20 mmol scale in an undivided cell with two platinum electrodes (each 1.0 x 1.0 cm^2). [b]*r.r* value was analyzed by ^1H NMR. [c]yields were determined by ^1H NMR using CH_2Br_2 as the internal standard. [d]The ee values were determined by chiral HPLC analysis. [e]The selectivity factor were calculated as s = ln[(1-C)(1-ee(**2a'**))]/ln[(1-C)(1+ee(**2a'**))], C = ee(**2a**)/(ee(**2a**)+ ee(**2a'**)). [f]Isolated yield.

We began our study by evaluating the performance of various chiral ligands on the kinetic resolution (KR) of diol **1a** in the presence of 4-benzoyloxy-substituted TEMPO **4** (10 mol%) as a mediator and $[Cu(MeCN)_4]OTf$ as a catalyst, with acetonitrile as the solvent, *n*-Bu_4NPF_6 as the electrolyte, and *N*-methyl imidazole (NMI) as the base in an undivided electrochemical cell (Table 1). Poor enantioselectivity and a low selectivity factor result when using bidentate pyridine bisoxazoline (PyBOX) ligand **L1**, although the conversion of **2a**/**3a** is excellent (entry 1). Gratifyingly, in the presence of BOX ligands bearing ^{i}Pr group (**L2**), the oxidative KR proceeds smoothly and affords product **2a** in 67% enantiomeric excess (ee) with **1a** recovered in 12% ee (entry 2). However, both the regioisomeric ration (r.r) of **2a**/**3a** and selectivity (*s*) factor are low (r.r = 88:12, *s* = 6). BOX ligands bearing phenyl (**L3**) or indane (**L4**) both afford **2a** in improved ee, and the ee values of recovered **1a** are also improved, but selectivity factors are still just 15 and 12 respectively, while regioselectivities are good to moderate (entries 3 and 4). Based on the hypothesis aforementioned, we synthesized a series of

TEMPO-BOX hybrid electrocatalysts（**E1-E5**） to enhance the proximity of the chiral center and the reactive site of **1a**.(*43*,*44*) (Table 1, For the synthesis of **E1**–**E5**, see Scheme S4-S8 in the Supporting Information for details). To our delight, indanyl **E1** affords **2a** in high enantioselectivity and regioselectivity (93% ee and >95:5 rr, respectively). The enantioselective excess of recovered **1a** is 92%, and the *s* factor is as high as 92 (entry 5). X-ray diffraction revealed the absolute configuration of **2a** to be *S*. Replacing the methyl group of **E1** with ethyl, isopropyl, or benzyl groups does not significantly improve the enantiomeric excess of **2a**. For example, ethyl-bearing ligand **E2** affords 84% ee and 23% yield of **2a** and 81% ee of recovered **1a** (entry 6). The oxidative KR proceeds smoothly in the presence of the isopropyl-bearing variant **E3**, affording **2a** in 91% ee and 47% yield with the recovery of **1a** in 82% ee and 52% yield (entry 7). Last in the indanyl series, benzyl-bearing **E4** affords a significantly decreased ee of **2a** and recovered **1a** (17% and 10% respectively, entry 8). Diphenyl-bearing analogue **E5** does not fare as well as **E1**, affording **2a** in 46% yield and 72% ee (in favor of the *R* enantiomer) (entry 9). The enantioselectivity of recovered **1a** is also low (68% ee) as is the selectivity factor.

With optimized conditions in hand, the functional group tolerance was evaluated to probe the efficiency of this bifunctional chiral ligand-enabled Cu-catalyzed electrochemical oxidative kinetic resolution (Table 2). Various 1,4-diols bearing substituted benzyl ethers (**1**) are well tolerated under the standard conditions, affording the corresponding lactones (**2**) and the enriched diols **2'** both in good enantioselectivities. For example, **1** bearing halogen, including Cl, Br, and I, afforded the corresponding lactones (**2b**–**2e**) in overall high enantioselectivity (93% to 98% ee) while the recovered 1,4-diols (**2b'**-**2e'**) are also well-enriched (87% to 97% ee). The selectivity factors are good or excellent (*s* = 91 to 419). Benzyl substituents bearing alkyl, naphthyl, and phenyl groups afford the corresponding lactones (**2f–2i**) with excellent enantioselectivity (93% to 97% ee), and high *s* factors (82 to 203). The recovered chiral diols (**2f–2i')** are also highly enriched (90% to 98% ee). Additionally, diols bearing heterocyclic analogues of benzyl ethers are also compatible with the protocol, providing the corresponding enantioenriched lactones **2j**–**2l** in excellent enantioselectivity (95% to 97%), with good regioselectivity (>94:6), and high *s* factors (180 to 203). To determine the absolute configuration of the recovered chiral 1,4-diols, we converted the diol **2k'** to the dibromide **4**, the absolute configuration of which was determined to be *R* by X-Ray diffraction analysis (Fig. 2A). It is worth noting that relatively sensitive functional groups including -PMP, -methylthio, -amine, -alkenyl, -alkynyl, are also tolerated in the presence of the bifunctional Cu-catalyzed systems, giving the corresponding lactones with good enantioselectivity, regioselectivity, and *s* factor (**2m**–**2s**). An analogue bearing an NHBoc group affords the corresponding lactone **2p** in excellent enantioselectivity (97% ee), and the recovered chiral diol **1p** is obtained in 91% ee and high selectivity factor of 314 (**2o** and **2p**, **2o'** and **2p'**). Excitingly, this bifunctional electrocatalyst also enables oxidative kinetic resolution of a cyclic 1,2-amino alcohol and an acyclic 1,3-amino alcohol, affording the corresponding amino aldehydes **2t** and **2u** and chiral protected amino alcohols **2t'** and **2u'** with good enantioselectivities and *s* factors.

Table 2. Enantioselective electrochemical lactonization of alcohols.[a-e]

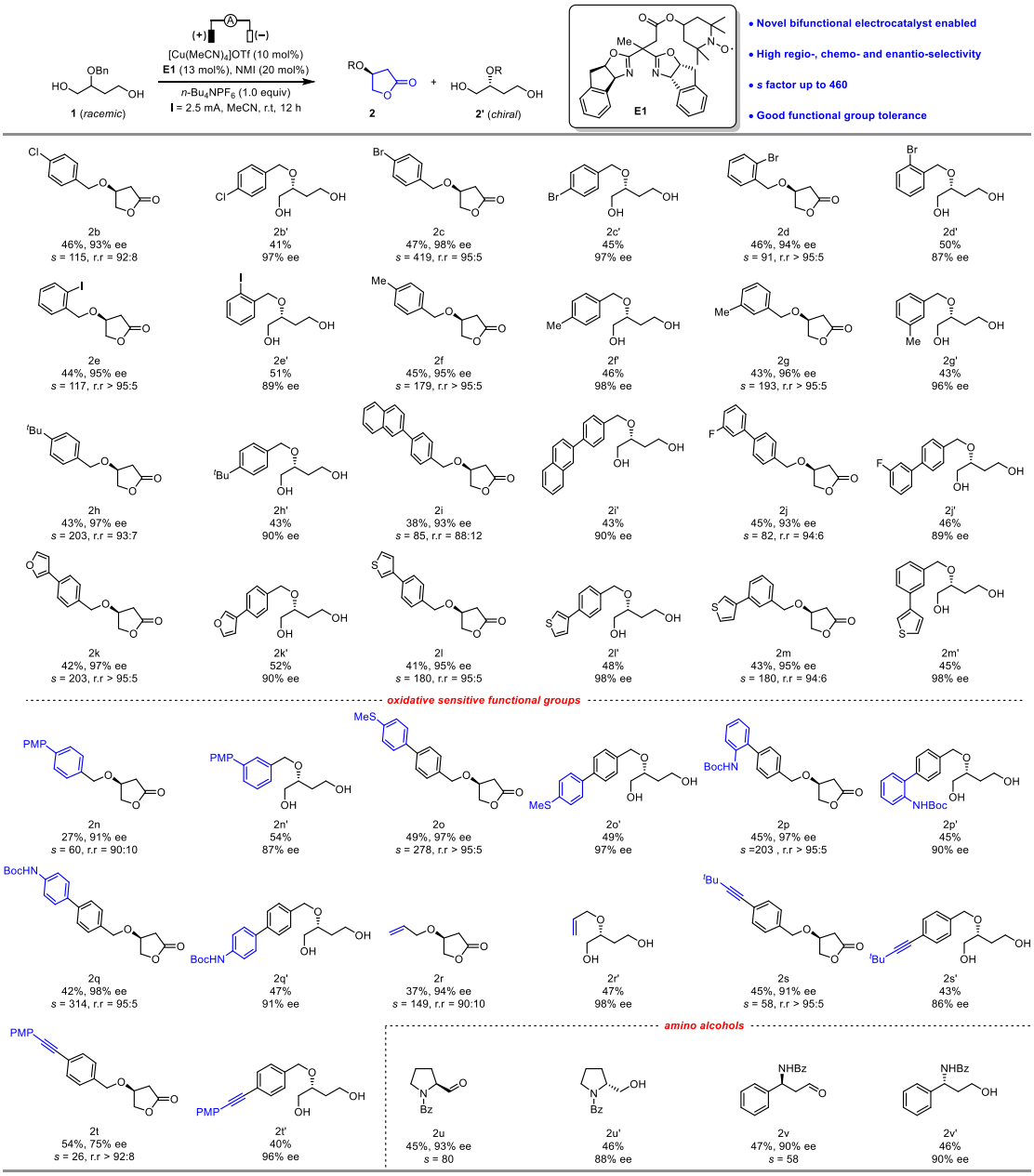

[a]Unless otherwise indication, the reaction was performed at 0.25 mmol scale in an undivided cell with two platinum electrodes (each 1.0 x 1.0 cm^2). [b]Isolated yields. [c]r.r value was analyzed by ^1H NMR. [d]The ee values were determined by chiral HPLC analysis. [e]The selectivity factor were calculated as $s = \ln[(1-C)(1-ee(\mathbf{2}'))]/\ln[(1-C)(1+ee(\mathbf{2}'))]$, $C = ee(\mathbf{2}')/(ee(\mathbf{2})+ ee(\mathbf{2}'))$.

We carried out several experiments to probe the reaction mechanism. Replacing the benzyl ether with a methyl group dramatically decreases enantioselectivity of the corresponding lactone **6**, suggesting that coordination of the OBn group to the copper catalyst is crucial for achieving good enantioselectivity (Fig. 2B). A parallel kinetic isotope effect (KIE) experiment comparing independent rates of reactions of **1c** and [d_6]-**1c** affords a primary KIE value (k_H/k_D) of 6.3. (Fig. 2C). This result indicates that

the abstraction of C–H is the rate-determining step and that the reaction involves a single electron transfer (SET) process.(*45*) To understand the effect of NMI, several cyclic voltammetric (CV) experiments were conducted. CV analysis of a mixture of **1a** and NMI indicate that NMI functions as a base. Both ligand **E1** and Cu(I)OTf exhibit a anodic feature at 0.47 V (red line, Fig. 2D) and 1.20V (blue line), respectively (vs $Ag/AgNO_3$). A mixture of Cu(I)OTf and **E1** exhibits an irreversible anodic CV feature at 0.77 V and 1.94 V (green line). The former peak is attributed to the oxidation of the TEMPO component to $TEMPO^+$ in **E1** (subsequently, $TEMPO^+$ may be responsible for the oxidation of Cu^+ complex to Cu^{2+}). The addition of 1.0 equivalent of substrate **1a** and NMI causes the anodic oxidative potential of **1a** (1.97 V vs $Ag/AgNO_3$) to be significantly shifted to 0.76V (yellow line). This large 1.2 V difference in potential suggests strong coordination of **1a** to Cu-**E1** in the course of oxidative lactonization. We also probed the existence of a non-linear effect to understand the Cu-**E1** coordination behavior.(*46*) The % ee of the ligand **E1** is linearly correlated to % ee of the resultant product (**2l**, in this case). The absence of non-linearity indicates that the

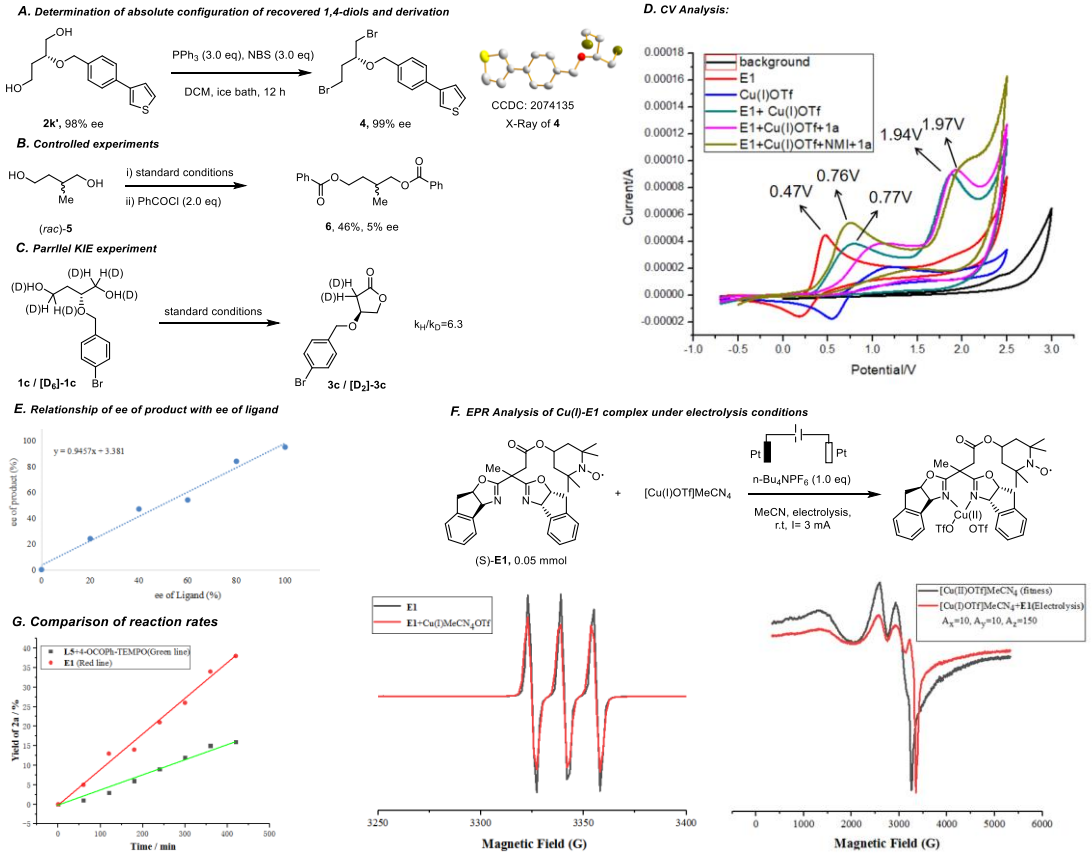

Fig. 2. Absolute Configuration Determination and Mechanistic study.

enantioselectivity-determining step might involve a single **E1** ligand and single Cu species (Fig. 2E). Electron paramagnetic resonance (EPR) analysis of Cu(I)-**E1** under electrolysis conditions exhibits signals resulting from both TEMPO and Cu(II), which is consistent with cooperative Cu(II)-**E1** catalysis (Fig. 2F). Notably, ligand **E1** performs more efficiently than when TEMPO and BOX are present but not linked. This was ascertained by conducting experiments on the relationship between the yield of **2a**

and electrolysis time in the presence of either ligand **E1 or L4**/4-OCOPh-TEMPO (green line, Fig. 2G). Interestingly, the reaction proceeds nearly twice as fast when using **E1** than when **L4** and 4-OCOPh-TEMPO are combined.

Although our mechanistic studies are far from comprehensive, a plausible catalytic cycle can be proposed based thereupon and in light of the reactivity trends. As shown in Fig. 3, active intermediate **T1** may be formed upon coordination of **E1** to precatalyst $[Cu(MeCN)_4]OTf$. Oxidized **T2** can then be accessed via either indirect TEMPO-involved (Path A involving **T3**) or direct (Path B) anodic oxidation. Intermediate **T4** is generated upon base-mediated coordination of the benzyl ether and hydroxyl groups of substrates **1a**. Subsequently, cooperative H• abstraction from the substrate via both Cu^{2+}–mediated oxidation and H atom transfer to TEMPO affords enantioenriched intermediate **Int 1**. After an intramolecular addition and another round of oxidation, product **2a** forms, with concomitant formation of double reduced species **T5**. Catalytic precursor **T1** is re-generated by anodic oxidation of **T5**.

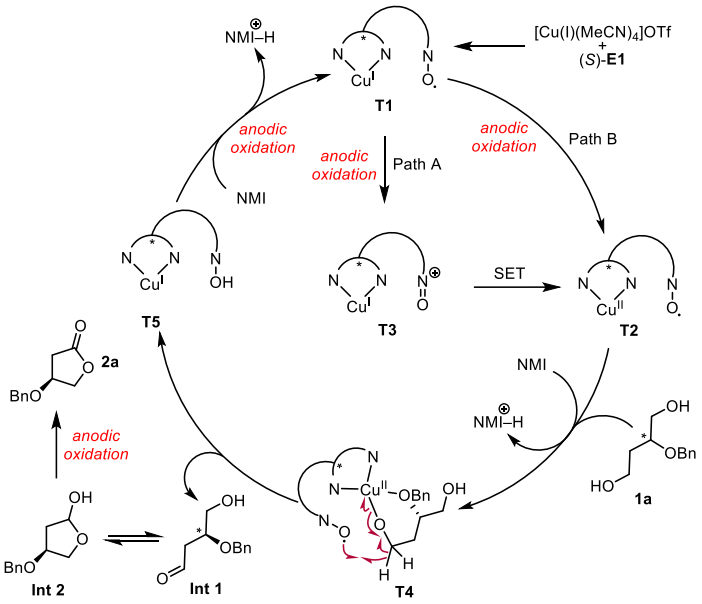

Fig. 3. Plausible catalytic cycle

In summary, we have discovered and developed a novel bifunctional chiral TEMPO-BOX ligand for copper electrocatalysts that enables a "two in one" strategy and developed a cooperative intramolecular Cu(II)-TEMPO oxidative strategy to achieve copper-catalyzed highly chemo-, regio-, and enantioselective electro-oxidative lactonizing kinetic resolution in an undivided cell. The electrocatalyst exhibits improved reaction selectivities and enhanced rates compared to catalytic reactions involving 'unlinked' BOX ligands and TEMPO. Further research to improve mechanistic understanding of this process and to achieve kinetic resolutions using green best practices is ongoing in our laboratory.

References and Notes

1. C. Zhu, N. W. J. Ang, T. H. Meyer, Y. Qiu, L. Ackermann, Organic Electrochemistry: Molecular Syntheses with Potential. *ACS Cent. Sci.* **7**, 415-431 (2021).
2. L. F. T. Novaes *et al.*, Electrocatalysis as an enabling technology for organic synthesis. *Chem. Soc. Rev.* **50**, 7941-8002 (2021).
3. C. Kingston *et al.*, A Survival Guide for the "Electro-curious". *Acc. Chem. Res.* **53**, 72-83 (2020).
4. B. R. Walker, S. Manabe, A. T. Brusoe, C. S. Sevov, Mediator-Enabled Electrocatalysis with Ligandless Copper for Anaerobic Chan–Lam Coupling Reactions. *J. Am. Chem. Soc.* **143**, 6257-6265 (2021).
5. T. Shen, T. H. Lambert, Electrophotocatalytic diamination of vicinal C–H bonds. *Science* **371**, 620-626 (2021).
6. X. Dong, J. L. Roeckl, S. R. Waldvogel, B. Morandi, Merging shuttle reactions and paired electrolysis for reversible vicinal dihalogenations. *Science* **371**, 507-514 (2021).
7. Y. Mo *et al.*, Microfluidic electrochemistry for single-electron transfer redox-neutral reactions. *Science* **368**, 1352-1357 (2020).
8. M. J. Chalkley, P. Garrido-Barros, J. C. Peters, A molecular mediator for reductive concerted proton-electron transfers via electrocatalysis. *Science* **369**, 850-854 (2020).
9. J. C. Siu, J. B. Parry, S. Lin, Aminoxyl-Catalyzed Electrochemical Diazidation of Alkenes Mediated by a Metastable Charge-Transfer Complex. *J. Am. Chem. Soc.* **141**, 2825-2831 (2019).
10. B. K. Peters *et al.*, Scalable and safe synthetic organic electroreduction inspired by Li-ion battery chemistry. *Science* **363**, 838-845 (2019).
11. W.-C. Gao, Z.-Y. Xiong, S. Pirhaghani, T. Wirth, Enantioselective Electrochemical Lactonization Using Chiral Iodoarenes as Mediators. *Synthesis* **51**, 276-284 (2019).
12. W. Fei, R. Mohammad, S. S. S., Electrochemical Functional-Group-Tolerant Shono-type Oxidation of Cyclic Carbamates Enabled by Aminoxyl Mediators. *Angew. Chem., Int. Ed.* **57**, 6686-6690 (2018).
13. N. Fu, G. S. Sauer, A. Saha, A. Loo, S. Lin, Metal-catalyzed electrochemical diazidation of alkenes. *Science* **357**, 575-579 (2017).
14. D. Amit, S. S. S., Noncovalent Immobilization of Molecular Electrocatalysts for Chemical Synthesis: Efficient Electrochemical Alcohol Oxidation with a Pyrene–TEMPO Conjugate. *Angew. Chem., Int. Ed.* **56**, 8892-8897 (2017).
15. E. J. Horn *et al.*, Scalable and sustainable electrochemical allylic C-H oxidation. *Nature* **533**, 77-81 (2016).
16. Y. Kashiwagi *et al.*, Enantioselective electrocatalytic oxidation of racemic amines using a chiral 1-azaspiro 5.5 undecane N-oxyl radical. *Chem. Commun.* 1983-1984 (1999).

17. F. Wang, S. S. Stahl, Electrochemical Oxidation of Organic Molecules at Lower Overpotential: Accessing Broader Functional Group Compatibility with Electron-Proton Transfer Mediators. *Acc. Chem. Res.* **53**, 561-574 (2020).
18. J. E. Nutting, M. Rafiee, S. S. Stahl, Tetramethylpiperidine N-Oxyl (TEMPO), Phthalimide N-Oxyl (PINO), and Related N-Oxyl Species: Electrochemical Properties and Their Use in Electrocatalytic Reactions. *Chem. Rev.* **118**, 4834-4885 (2018).
19. R. Francke, R. D. Little, Redox catalysis in organic electrosynthesis: basic principles and recent developments. *Chem. Soc. Rev.* **43**, 2492-2521 (2014).
20. X. Wang, X. Xu, Z. Wang, P. Fang, T.-S. Mei, Advances in Asymmetric Organotransition Metal-Catalyzed Electrochemistry. *Chin. J. Org. Chem.* **40**, 3738-3747 (2020).
21. K. Yamamoto, M. Kuriyama, O. Onomura, Anodic Oxidation for the Stereoselective Synthesis of Heterocycles. *Acc. Chem. Res.* **53**, 105-120 (2020).
22. X. Chang, Q. Zhang, C. Guo, Asymmetric Electrochemical Transformations. *Angew. Chem., Int. Ed.* **59**, 12612-12622 (2020).
23. Q. Lin, L. Li, S. Luo, Asymmetric Electrochemical Catalysis. *Chem. Eur. J.* **25**, 10033-10044 (2019).
24. Y. Gao *et al.*, Electrochemical Nozaki–Hiyama–Kishi Coupling: Scope, Applications, and Mechanism. *J. Am. Chem. Soc.* **143**, 9478-9488 (2021).
25. H. Qiu *et al.*, Enantioselective Ni-Catalyzed Electrochemical Synthesis of Biaryl Atropisomers. *J. Am. Chem. Soc.* **142**, 9872-9878 (2020).
26. P.-S. Gao *et al.*, CuII/TEMPO-Catalyzed Enantioselective C(sp3)–H Alkynylation of Tertiary Cyclic Amines through Shono-Type Oxidation. *Angew. Chem., Int. Ed.* **59**, 15254-15259 (2020).
27. U. Dhawa *et al.*, Enantioselective Pallada-Electrocatalyzed C-H Activation by Transient Directing Groups: Expedient Access to Helicenes. *Angew. Chem., Int. Ed.* **59**, 13451 (2020).
28. Q. Zhang, X. Chang, L. Peng, C. Guo, Asymmetric Lewis Acid Catalyzed Electrochemical Alkylation. *Angew. Chem., Int. Ed.* **58**, 6999-7003 (2019).
29. T. J. DeLano, S. E. Reisman, Enantioselective Electroreductive Coupling of Alkenyl and Benzyl Halides via Nickel Catalysis. *ACS Catal.* **9**, 6751-6754 (2019).
30. H. Tanaka, M. Kuroboshi, H. Takeda, H. Kanda, S. Torii, Electrochemical asymmetric epoxidation of olefins by using an optically active Mn-salen complex. *J. Electroanal. Chem.* **507**, 75-81 (2001).
31. S. Torii, P. Liu, N. Bhuvaneswari, C. Amatore, A. Jutand, Chemical and electrochemical asymmetric dihydroxylation of olefins in I_2-K_2CO_3-$K_2OsO_2(OH)_4$ and I_2-K_3PO_4/K_2HPO_4-$K_2OsO_2(OH)_4$ systems with Sharpless' ligand. *J. Org. Chem.* **61**, 3055-3060 (1996).
32. A. Badalyan, S. S. Stahl, Cooperative electrocatalytic alcohol oxidation with electron-proton-transfer mediators. *Nature* **535**, 406-410 (2016).

33. J. M. Hoover, B. L. Ryland, S. S. Stahl, Mechanism of Copper(I)/TEMPO-Catalyzed Aerobic Alcohol Oxidation. *J. Am. Chem. Soc.* **135**, 2357-2367 (2013).
34. X. Huang, Q. Zhang, J. Lin, K. Harms, E. Meggers, Electricity-driven asymmetric Lewis acid catalysis. *Nat. Catal.* **2**, 34-40 (2019).
35. W. Ding *et al.*, Bifunctional Photocatalysts for Enantioselective Aerobic Oxidation of β-Ketoesters. *J. Am. Chem. Soc.* **139**, 63-66 (2017).
36. H. Huo *et al.*, Asymmetric photoredox transition-metal catalysis activated by visible light. *Nature* **515**, 100-103 (2014).
37. A. Bauer, F. Westkämper, S. Grimme, T. Bach, Catalytic enantioselective reactions driven by photoinduced electron transfer. *Nature* **436**, 1139-1140 (2005).
38. X. Xie, S. S. Stahl, Efficient and Selective Cu/Nitroxyl-Catalyzed Methods for Aerobic Oxidative Lactonization of Diols. *J. Am. Chem. Soc.* **137**, 3767-3770 (2015).
39. H. Shimizu, S. Onitsuka, H. Egami, T. Katsuki, Ruthenium(salen)-Catalyzed Aerobic Oxidative Desymmetrization of meso-Diols and Its Kinetics. *J. Am. Chem. Soc.* **127**, 5396-5413 (2005).
40. Y. Kashiwagi *et al.*, Asymmetric electrochemical lactonization of diols on a chiral 1-azaspiro 5.5 undecane N-oxyl radical mediator-modified graphite felt electrode. *Chem. Commun.* 114-115 (2003).
41. Y. Yoshinori *et al.*, Enantioselective, Electrocatalytic Lactonization of Methyl-substituted Diols on a TEMPO-modified Graphite Felt Electrode in the Presence of (−)-Sparteine. *Chem. Lett.* **25**, 1043-1044 (1996).
42. Z. Ma, Q. Huang, J. M. Bobbitt, Oxoammonium salts. 5. A new synthesis of hindered piperidines leading to unsymmetrical TEMPO-type nitroxides. Synthesis and enantioselective oxidations with chiral nitroxides and chiral oxoammonium salts. *J. Org. Chem.* **58**, 4837-4843 (1993).
43. S.-H. Liao, X.-L. Sun, Y. Tang. Side Arm Strategy for Catalyst Design: Modifying Bisoxazolines for Remote Control of Enantioselection and Related. *Acc. Chem. Res.* **47**, 2260-2272 (2014).
44. Q.-J. Liu, L. Wang, Q.-K. Kang, X.-P. Kang, X.-P. Zhang, Y. Tang. Cy-SaBox /Copper (II)-Catalyzed Highly Diastereo- and Enantioselective Synthesis of Bicyclic N, O Acetals. *Angew. Chem., Int. Ed.* **55**, 9220-9223 (2016).
45. E. M. Simmons, J. F. Hartiwig, On the Interpretation of Deuterium Kinetic Isoptope Effects in C-H Bond Functionalizations by Transition Metal Complexes. *Angew. Chem., Int. Ed.* **51**, 3066-3072 (2012).
46. T. Satyanarayana, S. Abraham, H. B. Kagan, Nonlinear Effects in Asymmetric Catalysis. *Angew. Chem., Int. Ed.* **48**, 456-494 (2009).

ACKNOWLEDGEMENTS

Funding: This work was financially supported by National Key R&D Program of China (No. 2021YFA1500100), the NSF of China (Grants 21821002, 21772222, 21801087, and 91956112), the S&TCSM of Shanghai (Grants 18JC1415600 and 20JC1417100), and Bayer AG (Germany). **Author contributions:** P.-S.G. and T.-S.M. designed the project and wrote the manuscript. P.-S.G., H.-L.L., Y.-L.H., K.-J.J., and C.M. performed all experiments. All authors analyzed the results. **Competing interests:** Authors declare that they have no competing interests. **Data and materials availability:** Crystallographic data are available free of charge from the Cambridge Crystallographic Database Centre (CCDC) under CCDC 2034091 (for **2a**, see also the x-ray crystallographic data section of the supplementary materials) and CCDC 2074135 (for **4**). All other characterization data are in the supplementary materials."

SUPPLEMENTARY MATERIALS

Materials and Methods

Figs. S1 to S23

Schemes S1 to S26

NMR and HPLC Data

References (*47–51*)